

Divided We Fall: Defending Against Adversarial Attacks via Soft-Gated Fractional Mixture-of-Experts with Randomized Adversarial Training

Mohammad Meymani, Roozbeh Razavi-Far

Computer Science, University of New Brunswick, Fredericton, E3B 5A3, Canada

Abstract

Machine learning is a powerful tool enabling full automation of a huge number of tasks without explicit programming. Despite recent progress of machine learning in different domains, these models have shown vulnerabilities when they are exposed to adversarial threats. Adversarial threats aim to hinder the machine learning models from satisfying their objectives. They can create adversarial perturbations, which are imperceptible to humans' eyes but have the ability to cause misclassification during inference. In this paper, we propose a defense system, which devises an adversarial training module within mixture-of-experts architecture to enhance its robustness against white-box evasion attacks. In our proposed defense system, we use nine pre-trained classifiers (experts) with ResNet-18 as their backbone. During end-to-end training, the parameters of all experts and the gating mechanism are jointly updated allowing further optimization of the experts. Our proposed defense system outperforms state-of-the-art MoE-based defenses under strong white-box FGSM and PGD evaluation on CIFAR-10 and SVHN.

Keywords: Adversarial Machine Learning, Mixture of Experts, Robustness, Ensemble Learning, Adversarial Training, and Evasion Attacks.

Email addresses: mohammad.meymani79@unb.ca (Mohammad Meymani), roozbeh.razavi-far@unb.ca (Roozbeh Razavi-Far)

1. Introduction

Machine learning (ML) is a cornerstone of artificial intelligence (AI), which has been widely used in numerous applications. In computer vision, it enables face recognition and video surveillance [1, 2]. In health care, it facilitates disease diagnosis, drug repurposing, and personalized treatments [3, 4]. In natural language processing (NLP), ML enhances the quality of language translation [5, 6]. ML also empowers Large Language Models (LLMs) for code-related tasks such as code generation and understanding [7]. In cybersecurity, ML eases threat detection and manages system’s vulnerabilities [8–10]. Moreover, ML also plays an important role in other domains such as finance, speech processing, recommendation systems, autonomous vehicles, among others. However, those wide range of applications of machine learning has introduced opportunities for adversaries to exploit natural vulnerabilities of these models and launch adversarial attacks to threaten the integrity, privacy, and availability of these models [11–14].

Adversarial machine learning (AML) is at intersection of cybersecurity and machine learning and aims to investigate attacks on machine learning models, and design defense systems to counter these attacks. The adversary may have some knowledge about the victim’s model and/or its training data, which facilitates the adversarial sample generation [11–13]. Figure 1 shows how an adversarial sample looks like on an MNIST [15] sample when the adversary has a perfect knowledge about the model’s parameters. Samples like this can cause model’s misclassification with a high confidence during test time.

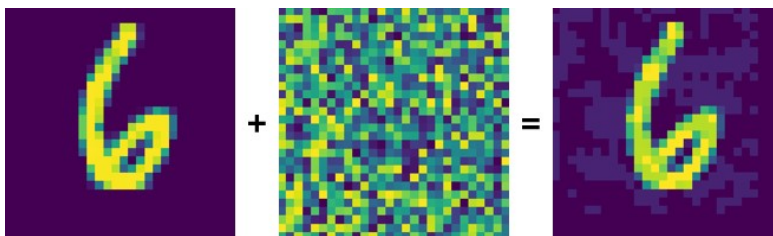


Figure 1: Generating an adversarial example on an MNIST digit by adding a carefully crafted perturbation, which remains imperceptible to humans but successfully fools the target models.

The rivalry between governments and industrial corporations has given rise to adversarial attacks causing global concerns about adversarial machine

learning. For instance, the government of United States of America has established Bipartisan AI task force, which are responsible for appropriate use of AI. They introduced AI guidelines such as accuracy, reliability, robustness, privacy, transparency, and safety. They also labeled generative and adversarial AI as a threat to privacy and confidentiality [16]. Moreover, the Department of Homeland Security (DHS) has considered evasion attacks and generative AI as a national threat violating security and privacy of individuals [17]. These insights highlight the need for secure AI systems and robust ML models.

Trustworthy AI is an important domain of AI ensuring that AI models remain lawful, ethical, robust, and efficient. Robust machine learning is an important branch in trustworthy AI which aims to make the machine learning models robust against adversarial threats while remain functional in non-adversarial environments [14]. Moreover, the main focus of Robust ML is to develop defense systems that detect and/or mitigate adversarial threats while preserving their efficiency and performance to a certain extent. These defense systems could either reside in the models or serve as an external entity protecting ML models [11–14].

Although adversarial machine learning encompasses multiple threat categories, including poisoning, model extraction, and privacy attacks, this study focuses specifically on inference-time robustness against white-box evasion attacks. Our evaluation therefore targets gradient-based adversarial examples generated with full model access. Training-time attacks and broader privacy or extraction threats are outside the scope of this work and are left for future investigation.

In pursuit of building a secure system, we build a novel defense system named Divided We Fall (DWF). In DWF, we employ Mixture of Experts (MoE) architecture which consists of benign and adversarial experts. The training scheme in DWF is joint, meaning that we do not freeze the weights of our pretrained experts during end-to-end training, which leads to stronger generalization capability of our proposed defense system improving the clean accuracy and robustness of our model. To ensure rigorous evaluation, robustness is assessed using strong white-box attacks, including properly tuned multi-step PGD with many iterations, multi-step restarts, and adaptive variants that optimize through the full mixture-of-experts architecture.

The proposed method is termed Divided We Fall to emphasize its distributed robustness principle. Rather than relying on a single monolithic classifier, which can be entirely compromised by adversarial perturbations, DWF decomposes the model into multiple specialized experts trained on

different regimes (benign, FGSM, and PGD). The soft gating mechanism adaptively combines their outputs at inference time, allowing the system to remain reliable even if individual experts are partially affected. By avoiding a single point of failure and encouraging specialization and cooperation, the overall model becomes more resilient to adversarial attacks.

Our contributions are as follows:

- Our proposed defense mechanism devises an adversarial training module within MoE, which outperforms related state-of-the-art defense systems in terms of both clean accuracy and robustness.
- Our model maintains high accuracy, while significantly outperforms undefended models in terms of robustness.
- We introduce a new training approach for MoE, where pretrained experts are jointly updated along with the gating mechanism during an end-to-end training session, where we use a mixed batch encompassing both benign and adversarial data.
- The randomized attack settings during all training stages enable DWF to generalize more efficiently in comparison to its competitors.

In Section 2, we illustrate the background problem setting. In Section 3, we introduce similar defense systems. In Section 4, we present the methodology and workflow of our defense. In Section 5, we demonstrate our experimental results. In Section 6, we investigate our proposed defense system limitations, potential future directions, and finally conclude our work.

2. Background and Problem Setting

In this section, we introduce MoE architecture and a background on adversarial threat model.

2.1. Mixture-of-Experts

MoE is an ensemble architecture using multiple experts, a gating mechanism to assign weights, and a router to aggregate results [18–20]. MoEs can be categorized based on their gating mechanism, routing topology, training strategy, and experts activation, which is shown in Figure 2.

Based on gating mechanism, MoE could be either soft or hard; in soft MoE the gating assigns non-zero weights to each expert forming fractional

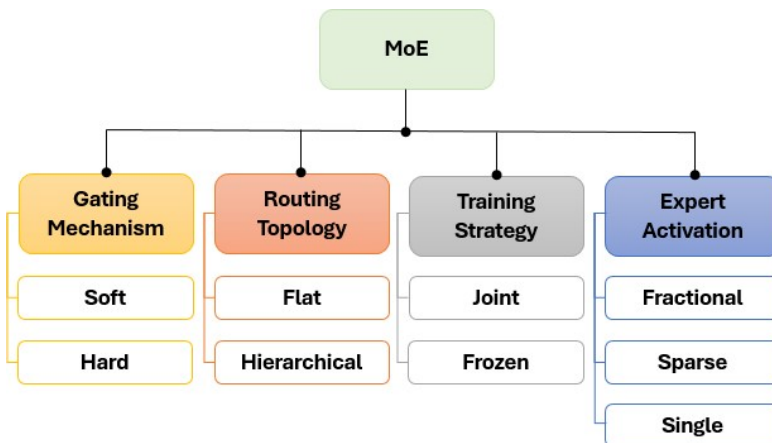


Figure 2: Main components and types of mixture of experts.

activation of experts, while in hard MoE, the gating mechanism chooses a subset of experts and assign wights to them making experts activation as sparse, or single if only one of them is chosen [18–20].

Training strategy could be either joint or frozen. In the first one, both router and experts are trained simultaneously, while the latter one uses pretrained experts and freezes their weights during training of the router [18–20].

Based on the routing topology we have flat and hierarchical routing schemes. In the flat MoE, all the experts reside in a single layer and the router chooses from them. In the hierarchical topology, the first router groups the experts into subgroups, and, then, the second one chooses some experts from these subgroups [18, 19, 21].

Using an expert-driven model allows for specialization within each part of the system, much like Unmanned Aerial Vehicle (UAVs) assigned specific roles within a swarm. These experts could respond dynamically to different types of attacks or threats, providing targeted defenses that are optimized for specific conditions, rather than relying on a single, monolithic defense mechanism [21].

2.2. General Adversarial Threat Models

Adversarial threats can be viewed from different angles: attacker’s knowledge, type, specificity, and objective.

2.2.1. Attacker's Knowledge

Attacker's knowledge shows the access level of the adversary to model's parameters, gradients, architecture, and training data. This knowledge is categorized into white-box, black-box, and gray-box based on the adversary's access level [11, 12].

White Box. Adversaries with white-box knowledge are the most effective and destructive attackers. These attackers have a full access to model's architecture, parameters, and gradients during training with full knowledge on the training data; this enables the attackers to generate adversarial samples based on the gradients and training data, which makes them very powerful. However, in a real-world scenario, adversaries can't achieve such an access, making them more suitable for research and testing the models' robustness [11, 12].

Black Box. In black-box scenario, unlike white-box, the adversaries have no knowledge about the model and the presence of any defense system. The adversaries can only give inputs and receive the corresponding outputs [11, 12, 22].

Gray Box. Gray box knowledge lies between white box knowledge and black box knowledge. The adversary has some degree of knowledge about the target system, which is not as perfect as white box, and is not as scarce as black box knowledge [11, 12].

2.2.2. Attacker's specificity

Based on specificity, each attack could either be targeted or untargeted. In targeted attacks, the adversary aims to degrade the model's performance when it faces specific patterns/inputs, while in untargeted attacks, also named to as indiscriminate, the goal is to cause any misclassification [11, 12].

2.2.3. Attacker's objective

Based on the objective, the adversary can follow degrade, breach, or both scenarios. In the first scenario, the adversary aims to harm the system's performance and/or violets its integrity. In breach, the adversary aims to explore the model in order to steal sensitive information, without affecting the model's performance [11, 12].

2.2.4. Attacker’s type

In a general perspective, an adversarial attack belongs to one of the following types: evasion, poisoning, backdoor, or physical layer attacks.

Evasion. An evasion attack targets the model at test time without affecting the system’s integrity on clean data. Evasion attacks are the most practical attack types aiming to degrade the model’s performance by causing misclassification during testing [11, 12, 23]. For instance attacks such as Fast Gradient Sign Method (FGSM) [24], Projected Gradient Descent (PGD) [25], and Carlini & Wagner (C&W) [26] make use of the model’s gradient during training to generate samples which evade the classifier during the test time. Equations 3 and 4, in Section 5, show how an adversarial sample is generated in FGSM and PGD, respectively.

Other Attack Types. Poisoning attacks compromise a model’s integrity by corrupting training data or embeddings, either through label manipulation or clean label attacks [11, 12, 27–30]. Exploratory attacks aim to violate privacy of the system. These attacks probe the target model to gain information about model’s parameters, training data, and algorithms on without affecting the performance and integrity of the model [31–33]. Moreover, physical attacks are launched on the models, which are deployed on a special physical hardware such as FPGA, GPU, and edge devices to exploit vulnerabilities emerged due to the increased attack surface in the physical layer [34, 35]. In this research work, we only focus on defending against evasion attacks to assess the resilience of our proposed approach under severe white-box attacks.

Figure 3 shows an overview of adversarial threat model.

All together, what we mentioned illustrates the seriousness of adversarial threats, highlighting the urge to build robust models to defend these adversarial threats, emphasizing the importance of adversarial machine learning and robust models.

3. Related Works

Given the arms race nature of adversarial machine learning, a plethora of attacks and defenses have been proposed and evolved over the years. This highlights the evolving nature of AML. In the following paragraphs, we investigate the related defenses in this area.

Adversarial training is a defense strategy aiming to train the model on both benign and adversarial samples to increase generalization capability of

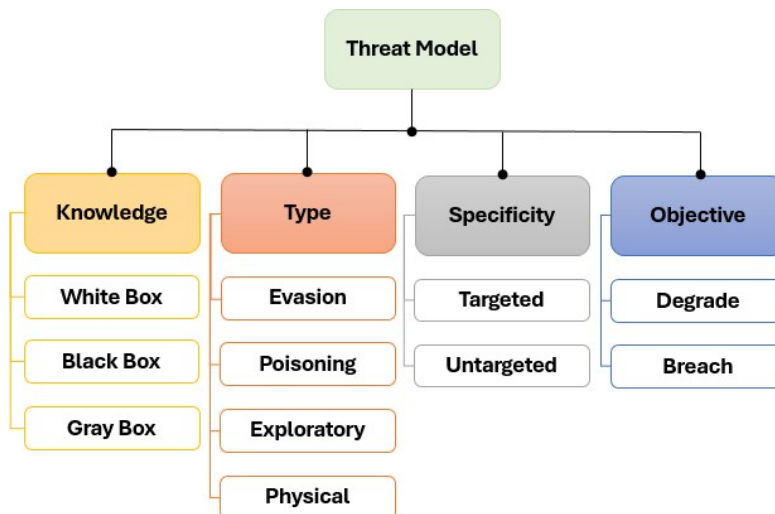


Figure 3: General taxonomy of the threat model.

the model enabling it to correctly predict both benign and adversarial inputs. However, this method often comes with a trade-off, where the model sacrifices its accuracy on the benign data to increase its robustness against adversarial inputs [36–39].

Adversarial training was first introduced in [24], which increased the model’s robustness against FGSM attacks by sacrificing the clean accuracy of the model. Methods such as TRadeoff-inspired Adversarial DEfense via Surrogate-loss minimization (TRADES) [40] and Fair Robust Learning (FRL) [41] have been introduced to control natural robustness-accuracy trade-off in adversarial training. Additionally, methods such as Fast Free Adversarial Training (FFAT) [42] tackles the computational overhead of adversarial sample generation, while having a lower accuracy and robustness in comparison to standard adversarial training.

Ensemble architectures have shown strong robustness against adversarial threats in comparison to the non-ensemble architectures. This is due to the natural complex architecture of ensemble models. Ensemble-based defense methods are categorized into distillation, hierarchical, and MoE.

Ensemble distillation-based defenses aim to harden the model by training it on soft labels and/or noisy logits instead of hard labeling, producing results via ensembles. Research works in this category include Distillation Hardening for Random Forest (DDH-RF) [43] and SELENA [44]. Hierarchical defenses,

on the other hand, aim to build ensemble of models in a hierarchical manner to detect and mitigate adversarial attacks in multiple levels, which make the defense systems robust against a wider range of attacks. Hierarchical defenses include Application Constraints (AppCon) [45], Model Stacking [46], and Ensemble Methods as a Defense (EMD) [47].

[48, 49] investigate the adversarial robustness of MoEs. In [50, 51], some defense systems are proposed, which aim to protect the architecture of MoEs. Defenses such as adversarial mixture-of-expert (ADVMoE) [52] and synergy-of-experts (SoE) [53] make use of the ensemble architecture of MoEs to defend against adversarial threats. Both ADVMoE and SoE use adversarial training techniques, while training their MoE to increase the robustness of their model.

Table 1 presents the differences between the category of MoE used in our defense system and other competitors.

Table 1: MoE type of DWF vs. other competitors - gating mechanism (GM), routing topology (RT), training strategy (TS), and experts activation (EA).

Defense	GM	RT	TS	EA
SoE	Hard	Flat	Joint	Single
ADVMoE	Hard	Flat	Joint	Sparse
DWF	Soft	Flat	Pre-trained+Joint	Fractional

While standard adversarial training methods improve robustness by augmenting training data with adversarial examples, they typically train a single model with a uniform objective. In contrast, our approach explicitly decomposes the problem into multiple specialized experts, each trained on different regimes (benign, FGSM, and PGD), and combines them via a soft gating mechanism. This distinguishes totally from conventional adversarial training, which lacks explicit expert specialization and input-dependent routing.

4. Methodology

Our defense uses soft and flat structure for MoE with fractional activation of experts. In the first phase of training, we independently train a classifier on benign data (benign expert), four classifiers on FGSM data (FGSM experts), and four classifiers on PGD data (PGD experts). This design encourages diversity among experts, which is a key principle in mixture-of-experts architectures. After this pretraining stage, we move to end-to-end

learning, in which the entire framework is jointly optimized. During this stage, for each batch of data, we generate adversarial variants of the inputs using both FGSM and PGD attacks, and augment them with the original benign inputs to form an expanded batch. This mixed batch preserves the diversity of benign and adversarial samples, enhancing the network’s robustness and generalization capability. Finally, the combined batch is fed into the network, so the whole framework learns both benign and adversarial patterns. Figure 4 shows an overview of our defense model’s workflow.

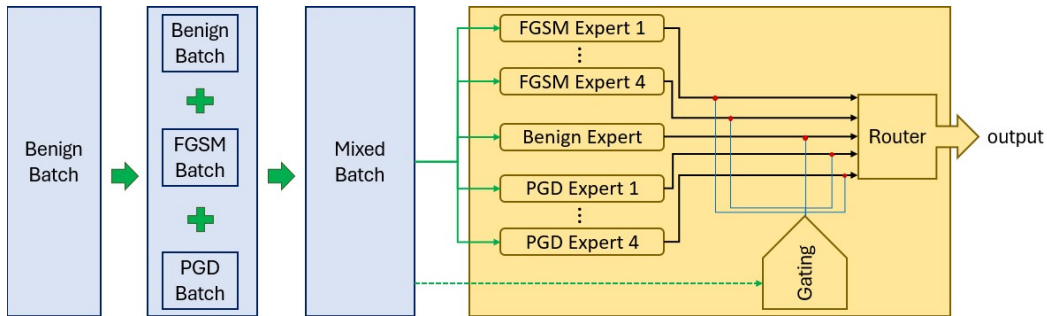


Figure 4: General view of the end to end training of our proposed defense system.

During training, we sample attack strengths (FGSM ϵ and PGD iterations) from a range rather than fixing a single configuration. This strategy prevents overfitting to a specific perturbation magnitude and exposes the model to adversarial examples of varying difficulty, improving robustness generalization across threat levels. Consequently, the model is not tuned to a particular evaluation ϵ but learns to remain stable under a spectrum of perturbations. A detailed ablation over all sampling ranges is left for future investigation due to computational cost.

To construct FGSM experts, we need to pre-train them before end-to-end training. During adversarial training of an FGSM expert, within every batch and each epoch we randomly assign a value between 0.01 to 0.09 to perturbation size ϵ , and the models is adversarially trained on random perturbation size during that epoch. This strategy helps to increase generalization ability of the network, making it more robust against different perturbation sizes. We train four models in this manner. Algorithm 1 shows how we train the FGSM experts.

We take the same strategy to train the PGD experts, with a minor difference. This time we alter the iterations number, and randomly choose a

Algorithm 1: Training FGSM Experts.

Input: Benign inputs: X , labels: Y , and number of epochs: E .
model \leftarrow Instantiate(ResNet-18);
for $e \in \{0, 1, \dots, E - 1\}$ **do**
 for $(x, y) \in (X, Y)$ **do**
 $\epsilon \leftarrow$ **Random**{0.01, 0.02, ..., 0.09};
 $x_{\text{adv}} \leftarrow x + \epsilon \cdot \text{sign}(\nabla_x L(\theta, x, y))$;
 $y_p \leftarrow$ model.forward(x_{adv});
 loss $\leftarrow \ell(y_p, y)$;
 model.backward(loss);
return model.

different iteration number within in each batch. With the same approach we train four PGD experts. Algorithm 2 shows how we train the PGD experts.

Algorithm 2: Training PGD Experts.

Input: Benign images: X , labels: Y , perturbation bound: ϵ , step size: α , and number of epochs: E .
model \leftarrow Instantiate(ResNet-18);
for $e \in \{0, 1, \dots, E - 1\}$ **do**
 for $(x, y) \in (X, Y)$ **do**
 iterations \leftarrow **Random**{10, 20, 30, 40, 50};
 $x_{\text{adv}} \leftarrow$ PGD(x, ϵ, α , iterations);
 $y_p \leftarrow$ model.forward(x_{adv});
 loss $\leftarrow \ell(y_p, y)$;
 model.backward(loss);
return model.

Now we have a benign expert, which is trained on benign data, four FGSM experts, and four PGD experts. To train the end-to-end framework, we do not freeze the parameters of the experts. During each batch we generate FGSM and PGD version of our input, with random perturbation size and iteration number, respectively. The batch size during this stage of training is three times larger than the batch size for training the experts, which includes benign input, FGSM inputs, and PGD inputs that together can enhance clean accuracy and robustness of the network. Algorithm 3 shows the end-to-end

training of our MoE network.

Algorithm 3: End-to-End Training of Mixture of Experts.

Input: Benign images: X , labels: Y , perturbation bound: ϵ , step size: α , number of epochs: E , and Experts: experts.

model \leftarrow Instantiate(mixture-of-expert);

model.add(experts);

for $e \in \{0, 1, \dots, E - 1\}$ **do**

for $(x, y) \in (X, Y)$ **do**

$\epsilon_{\text{FGSM}} \leftarrow \mathbf{Random}\{0.01, 0.02, \dots, 0.09\}$;

$x_{\text{FGSM}} \leftarrow x + \epsilon_{\text{FGSM}} \cdot \text{sign}(\nabla_x L(\theta, x, y))$;

 iterations $\leftarrow \mathbf{Random}\{10, 20, 30, 40, 50\}$;

$x_{\text{PGD}} \leftarrow \text{PGD}(x, \epsilon, \alpha, \text{iterations})$;

$x_{\text{mixed}} = \text{Concatenate}(x, x_{\text{FGSM}}, x_{\text{PGD}})$;

$y_p \leftarrow \text{model.forward}(x_{\text{mixed}})$;

$y_{\text{mixed}} = \text{Concatenate}(y, y, y)$;

 loss $\leftarrow \ell(y_p, y_{\text{mixed}})$;

 model.backward(loss);

return model.

After all these training stages, the model is ready for testing and deployment. During both phases, DWF uses fractional schema for the experts, which enables them to contribute in the final decision. Final decision is made as follows:

$$y = \sum_{i=1}^n w_i(x) \cdot f_i(x) \quad (1)$$

where n is the number of experts, $w_i(x)$ is the gating weights, and $f_i(x)$ stands for the i_{th} expert.

The gating function is implemented as a lightweight learnable router that takes the same input x as the experts and produces a soft assignment vector using a small multilayer perceptron followed by a softmax normalization. The final prediction is obtained via a weighted sum of all expert logits (soft routing), rather than hard or sparse selection. All experts and the gating network are trained jointly in an end-to-end manner using the standard cross-entropy loss. No auxiliary routing objectives, load-balancing losses, temperature scaling, or sparsity regularization are used. This simple design avoids additional hyperparameters and improves reproducibility.

The weights $w_i(x)$ in (1) are generated by a learnable gating network $g(\cdot)$. Given an input x , the gating network produces a score vector $s(x) \in \mathbb{R}^n$, which is normalized using a softmax function to obtain non-negative weights that sum to one:

$$w_i(x) = \frac{e^{s_i(x)}}{\sum_{j=1}^n e^{s_j(x)}} \quad (2)$$

The gating network is trained jointly with all experts during end-to-end training by backpropagating the cross-entropy loss through both the experts and the gating mechanism. Thus, $w(x)$ is not fixed or heuristic, but learned from data in an input-dependent manner.

During training, we randomize attack parameters such as perturbation magnitude and step size. This randomness is not strictly required for robustness, but is used to increase perturbation diversity and avoid overfitting to a single fixed attack configuration. By exposing the experts to a wider range of adversarial strengths, the model generalizes better to unseen attacks. In practice, similar behavior can still be achieved with fixed parameters, although randomized training typically provides slightly more stable robustness.

The number of experts determines a trade-off between robustness and computational cost. A larger number of experts enables greater specialization to different input regimes, which can improve robustness. However, both memory and inference cost grow approximately linearly with the number of experts, while the marginal gain diminishes as experts begin to learn overlapping representations. Therefore, we adopt nine experts as a practical compromise that provides strong robustness while maintaining reasonable computational efficiency.

All experts share the same backbone architecture (ResNet-18) in our implementation. This choice is intentional to ensure fair comparisons and to isolate the contribution of the proposed soft-gated mixture-of-experts training strategy, rather than improvements arising from heterogeneous model capacities. Despite identical architectures, diversity is still achieved through specialization: each expert is trained on different input regimes (benign and adversarial attacks), which results in distinct decision boundaries and complementary behaviors. Incorporating heterogeneous backbones could further increase diversity and potentially improve robustness; however, this would introduce additional computational cost and confounding factors. Exploring architectural diversity among experts is an interesting direction for future work.

5. Experiments

In this section, we firstly describe the hardware type and software libraries used in our experiments. Then, we present the dataset, target models, and adversarial attacks considered. Next, we provide details on the normalization procedure employed during both training and test phases. We also explain the learning settings used in our proposed defense system. Finally, we introduce the evaluation metrics and demonstrate the attained results.

Table 2: Accuracy and robustness of our proposed defense system vs. other models in terms of standard accuracy (SA) and robust accuracy (RA) (FGSM) - DenseNet-169 (DN169).

Model	Metric	RA - FGSM								
	SA	0.01	0.02	0.03	0.04	0.05	0.06	0.07	0.08	0.09
CIFAR-10										
VGG-19	93.18	52.08	50.92	48.52	41.53	29.22	20.22	16.06	13.70	12.00
ResNet-18	92.35	52.32	48.19	40.97	30.28	21.38	15.61	12.72	11.61	11.00
ResNet-18 (FGSM-AT)	89.22	78.81	67.50	48.37	32.71	23.52	16.48	12.2	9.54	9.26
ResNet-18 (PGD-AT)	87.99	78.83	64.29	41.46	28.34	20.8	15.29	11.57	9.8	9.78
ResNet-50	95.29	52.68	51.54	46.01	35.04	25.46	19.26	16.25	13.87	12.14
DN169	95.10	55.32	54.57	48.63	36.38	25.21	18.57	15.00	12.88	11.90
GoogLeNet	95.01	53.83	51.53	46.96	33.59	22.70	16.61	13.83	11.69	10.91
Inception-V3	94.78	58.00	56.77	52.05	41.99	29.99	21.89	16.53	13.61	11.97
Xception	93.48	51.41	50.20	47.69	37.72	26.35	18.45	14.21	12.32	10.96
MobileNet-V2	94.20	55.05	53.79	49.31	36.67	24.70	18.31	15.38	13.39	12.19
SoE	81.69	70.23	66.22	60.27	52.65	44.62	38.26	32.96	28.74	25.74
ADVMoE	88.27	79.39	62.09	40.88	23.90	16.53	15.47	15.98	16.07	16.40
DWF (Ours)	91.19±0.43	82.83±0.2	79.66±0.37	74.76±0.96	69.01±1.37	63.6±1.52	58.40±1.55	52.97±1.17	47.34±0.63	41.24±0.42
SVHN										
ResNet-18	95.95	70.98	67.85	63.03	54.87	46.20	35.59	25.96	18.29	13.77
ResNet-34	96.26	70.54	67.2	63.12	57.53	48.74	38.74	28.38	19.89	14.6
ResNet-50	96.32	69.02	66.75	63.03	57.98	50.81	41.39	31.33	22.6	16.62
DenseNet-121	95.53	70.36	66.87	61.52	56.2	48.94	40.74	32.36	25.09	19.97
ADVMoE	88.88	79.22	62.87	41.69	24.71	15.86	14.05	14.05	13.47	13.42
DWF (Ours)	92.35±0.36	81.43±0.22	78.02±0.42	74.88±0.99	68.94±1.59	63.1±1.36	57.53±1.68	52±1.03	47.73±0.81	41.3±0.54

Hardware and Implementation. All experiments were conducted on a server equipped with two NVIDIA H100 GPUs each with 80 GB of VRAM, and 512 GB of RAM, offering the adequate computational power for MoE training. While we used two NVIDIA H100 GPUs to accelerate experimentation, the proposed DWF architecture is composed of lightweight ResNet-18 experts and is modular. Training can be performed on more modest GPU environments by reducing batch size and/or using gradient accumulation; additional ablations on scaling with fewer experts are left for future work. Importantly, inference is substantially cheaper than training and can be deployed on commodity GPU hardware. We implemented all the code in PyTorch with torch 2.7.1 and torchvision 0.22.0, and CUDA 12.8.

DWF introduces additional computational overhead compared to single-network baselines due to the joint training and inference of multiple experts. On our hardware, full training requires several days (approximately five

Table 3: Accuracy and robustness of our proposed defense system vs. other models in terms of PGD robust accuracy.

Metric Model	RA - PGD						
	10	20	30	40	50	100 (MS)	100 (A)
CIFAR-10							
VGG-19	42.66	41.91	41.72	41.80	41.80	41.52	41.7
ResNet-18	37.72	37.28	37.10	37.02	36.95	37.07	37
ResNet-18 (FGSM-AT)	58.65	58.21	58.17	58.14	58.13	58	58.11
ResNet-18 (PGD-AT)	58.74	58.35	58.31	58.26	58.26	58.05	58.26
ResNet-50	46.20	45.68	45.53	45.44	45.45	44.86	45.39
DenseNet-169	47.55	46.99	46.81	46.72	46.81	45.72	46.73
GoogLeNet	39.60	38.59	38.53	38.48	38.49	38.34	38.39
Inception-V3	47.21	45.51	45.01	44.68	44.80	43.66	44.55
Xception	41.36	40.58	40.44	40.30	40.30	40.01	40.31
MobileNet-V2	45.77	45.20	45.14	45.17	45.08	45.03	45.12
SoE	62.27	62.34	62.31	62.31	62.31	62.03	62.27
ADVMoE	47.69	44.95	44.36	44.11	44.01	42.47	43.49
DWF (Ours)	65.51±0.93	64.7±1.08	64.52±1.1	64.42±1.08	64.37±1.1	64.2±1.15	64.32±1.12
SVHN							
ResNet-18	49.61	48.86	48.62	48.56	48.52	48.29	48.46
ResNet-34	49.04	48.04	47.83	47.71	47.66	47.37	47.54
ResNet-50	48.74	47.88	47.7	47.6	47.54	47.25	47.45
DenseNet-121	45.94	44.54	44.29	44.18	44.14	43.82	44.05
ADVMoE	47.22	44.22	43.31	43	42.68	8.13	8.33
DWF (Ours)	64.93±1.04	64.08±1.03	63.97±1.19	63.92±1.21	63.88±1.21	63.69±1.37	63.78±1.29

days of wall-clock time, corresponding to roughly 240 GPU-hours), whereas single baselines complete substantially faster. ADVMoE and SoE exhibit intermediate training costs between these extremes. During inference, the gating module is lightweight and the dominant cost comes from evaluating the experts, resulting in approximately linear scaling with the number of experts. Although DWF is computationally heavier than plain networks, we find the overhead acceptable in practice given the considerable robustness gains. This highlights a typical robustness-efficiency trade-off.

Datasets. To conduct our experiments, we use CIFAR-10 [54] and street view house number (SVHN) [55] datasets, which are RGB-colored datasets, each include 10 labels.

Attacks. In order to train our model and test its robustness, we employ FGSM and PGD. FGSM is a single step attack, which generates adversarial samples using the following formula:

$$x_{adv} = x + \epsilon \cdot \text{sign}(\nabla_x \ell(\theta, x, y)) \quad (3)$$

where x is benign input, y is the label, x_{adv} is the perturbed version of x , ϵ is perturbation size, sign returns the sign of the input, θ denotes the model’s parameters and $\nabla_x \ell(\theta, x, y)$ is the gradient of loss function with respect to x .

PGD, on the other hand, is an iterative attack, computing the final version of adversarial samples iteratively:

$$x_{adv}^{i+1} = \prod_{x+\epsilon} (x_{adv}^i + \alpha \cdot \text{sign}(\nabla_x \ell(\theta, x, y))) \quad (4)$$

where α is step size, i is the iteration number, x_{adv}^i is the perturbed sample during the i_{th} iteration, and $\prod_{x+\epsilon}$ ensures each generated adversarial sample remains within ϵ perturbation bound during each iteration. The formula for $\prod_{x+\epsilon}$ is as follows:

$$x_{adv} = \begin{cases} x_{adv} & \text{if } x - \epsilon \leq x_{adv} \leq x + \epsilon \\ x + \epsilon & \text{if } x_{adv} > x + \epsilon \\ x - \epsilon & \text{if } x_{adv} < x - \epsilon \end{cases} \quad (5)$$

Moreover, to further assess the resilience of our proposed approach, we conduct further experiments under white-box multi-step PGD and adaptive PGD attacks.

Table 4: Attacks settings - expectation over transformation (EoT).

Attacks	Settings	Attacker's Knowledge	Defense's Knowledge
FGSM	$\epsilon \in \{0.01, 0.02, \dots, 0.09\}$	white-box	white-box
PGD	$\epsilon = \frac{8}{255}, \alpha = \frac{2}{255}, i \in \{10, 20, 30, 40, 50\}$	white-box	white-box
Multi-Step PGD	$\epsilon = \frac{8}{255}, \alpha = \frac{2}{255}, i = 100, \text{Restart} = 3$	white-box	black-box
Adaptive PGD	$\epsilon = \frac{8}{255}, \alpha = \frac{2}{255}, i = 100, \text{EoT Samples} = 1$	white-box	black-box

Table 5: Hyper parameters - learning rate (LR), batch size (BS), and weight decay (WD).

Models	Epochs	LR	BS	WD
Experts	150, 100	0.01	128, 128 × 3	5e − 4
Gating	100	0.01	128 × 3	5e − 4
End2End	100	0.01	128 × 3	5e − 4

Benign baselines. To compare our results with plain networks we used networks pretrained on CIFAR-10 from [56, 57] and networks pretrained on SVHN from [58]. These models include VGG-19 [59], ResNet-34, ResNet-50 [60], DenseNet-121, DenseNet-169 [61], GoogLeNet, Inception-V3 [62], Xception [63], and MobileNet-V2 [64].

Plain-network baselines are initialized from standard publicly available pretrained checkpoints. Although their original training recipes may differ slightly, all models are evaluated under an identical test-time protocol, including the same preprocessing, normalization, and attack settings, ensuring controlled robustness comparisons. These checkpoints achieve strong clean accuracy, indicating that they are competitive baselines rather than undertrained variants. The substantial robustness gap observed between our method and these baselines suggests that minor differences in the original training procedures are unlikely to affect the main conclusions. The attained results are shown in Table 3.

Adversarially trained baselines. To evaluate whether the observed resilience stems from the adversarial training schedule, the ensemble structure, or a combination of both, we conducted adversarial training experiments with two separate ResNet-18 models using different adversarial training methods: FGSM and PGD.

Backbone. For every expert we use ResNet-18 [60] as the backbone architecture, since other relevant defenses use the same backbone. Figure 5 shows the backbone details.

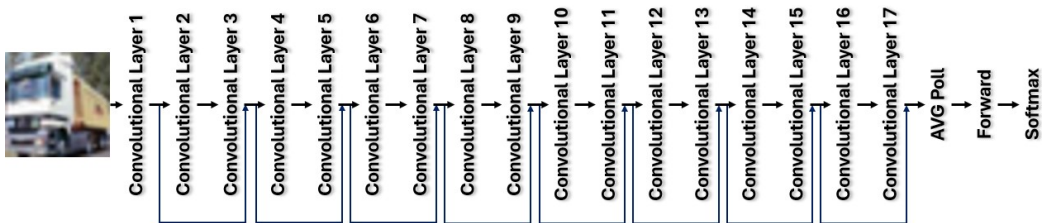


Figure 5: The backbone architecture of DWF network.

Threat Model. We adopt a full white-box threat model where the adversary has complete knowledge of the entire DWF architecture, including all experts, the gating network, and routing weights. Gradients are computed through the

full mixture-of-experts pipeline, allowing attacks to jointly optimize perturbations with respect to both expert predictions and gating behavior. Therefore, the attacker explicitly targets the complete MoE routing mechanism rather than individual experts only. To further approximate worst-case adversarial conditions, we additionally evaluate stronger multi-step and adaptive attacks that account for input-dependent routing, ensuring that the robustness assessment is not affected by gradient masking or routing-specific obfuscation.

To evaluate our model’s resilience against white box attacks, we employ FGSM with the perturbation sizes $\epsilon \in \{0.01, 0.02, \dots, 0.09\}$, and PGD with the step size $\alpha = \frac{2}{255}$, perturbation bound $\epsilon = \frac{8}{255}$, and iterations numbers $i \in \{10, 20, 30, 40, 50\}$. These settings were used during both training and test phases, highlighting that both threat model and defense system have white-box knowledge about each other. Moreover, to further evaluate our proposed defense’s performance against unseen attacks (black-box defense knowledge), we used multi-step PGD-100 with 3 restarts and adaptive PGD-100 with expectation over transformation (EoT) of one. Table 4 shows an overview of the attacks settings.

Normalization Procedure. Let $x \in [0, 1]^{32 \times 32 \times 3}$ be an RGB image sample from CIFAR-10. The normalization procedure for each of the three channels is as follows:

$$x'_c(i, j) = \frac{x_c(i, j) - \mu_c}{\sigma_c} \quad (6)$$

where $c \in \{R, G, B\}$ stands for each color channel, x'_c is the normalized version of x_c , μ_c is the empirical mean over channel c , σ_c is the empirical deviation over channel c , and i, j are row index and column index, respectively. To normalize CIFAR-10 data we defined $\mu = (0.4377, 0.4438, 0.4728)$ and $\sigma = (0.1980, 0.2010, 0.1970)$. Moreover, to normalize SVHN data we defined $\mu = (0.4914, 0.4822, 0.4465)$ and $\sigma = (0.2023, 0.1994, 0.2010)$.

Learning Settings. We trained all the experts over 150 epochs using batch size of 128. We used stochastic gradient descent as the optimizer with an initial learning rate of 0.01, momentum of 0.9, and weight decay of $5e^{-4}$. During the training session of the end to end framework, all the models are retrained as well as the gating mechanism for 100 epochs with batch size of 128×3 , where the first part includes benign inputs, the second and the third include the corresponding FGSM and PGD inputs, respectively. We also used the cross-entropy loss as the loss function for training.

Additionally, to further improve our model’s stability, we employed a cosine annealing learning rate scheduler [65] to decay the learning rate gradually over all iterations in all training sessions. Table 5 shows an overview of the hyper parameters used for training our proposed approach.

ADVMoE used TRADES [40] as the adversarial training objective by adopting PGD with attack strength of $\epsilon = \frac{8}{255}$ during two iterations. Additionally, it was trained during 200 epochs with learning rate of 0.1, momentum of 0.9, weight decay of $5e^{-4}$, and batch size of 128. SoE was adversarially trained during 200 epochs with learning rate of 0.1 and batch size of 128. The first ResNet-18 model was adversarially trained using the FGSM with a perturbation magnitude of $\epsilon = 0.03$, where half of each training batch consisted of FGSM-generated adversarial examples. The second ResNet-18 model was trained using PGD, with the adversarial perturbation set to $\epsilon = \frac{8}{255}$, step size $\alpha = \frac{2}{255}$, and 10 iteration, where half of each training batch consisted of PGD-generated adversarial examples.

To ensure fair comparisons, all methods use the same backbone architecture (ResNet-18), optimizer, learning rate schedule, and training protocol. Some baselines (e.g., ADVMoE and SoE) also employ multiple experts, although the number of experts varies across methods as part of their architectural design. A larger number of experts increases computational cost, analogous to increasing network width or depth, and should therefore be interpreted as a capacity trade-off rather than an advantage in training settings. Our comparisons keep the optimization procedure identical while allowing each method to retain its original architecture.

Metrics. To compare our model with other models, we use two metrics called standard accuracy (SA) and robust accuracy (RA). The first metric measures the model’s accuracy on the benign data, while the latter one measures the models accuracy on the adversarial data.

Results. Table 3 illustrates the accuracy and robustness of our proposed model in comparison with other models. Figures 6 and 7 present a visual summary of the results reported in Table 3 and provide clearer comparison between our proposed model and other competitors in terms of robust accuracy under different settings for FGSM and PGD attacks. The attained results by our model are averaged over five runs, ensuring a fair comparison.

To isolate architectural effects from training-related factors, all compared defended methods, including ADVMoE and SoE, are trained and evaluated

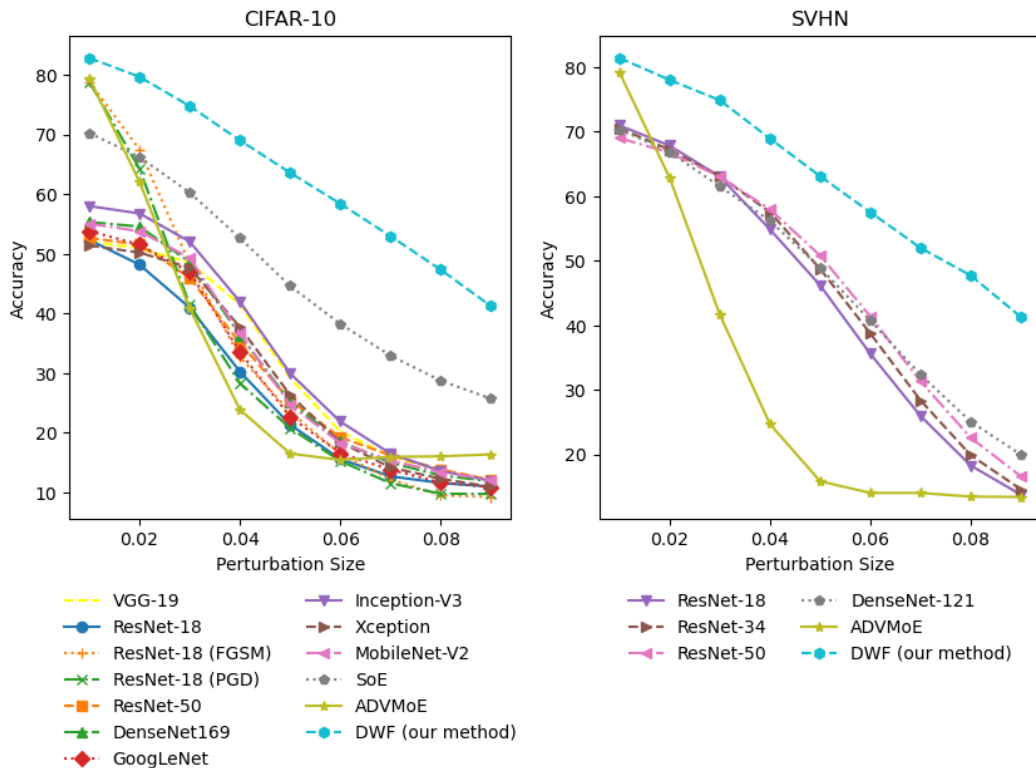


Figure 6: Robustness of our proposed model compared with the other competitors against FGSM w.r.t. different perturbation sizes.

under the same experimental pipeline with identical preprocessing, backbone configuration, and optimization protocol. Robust accuracy is computed using the same threat models for every method. Consequently, performance differences primarily reflect differences in architectural design rather than inconsistencies in training or evaluation procedures.

The results over these runs vary slightly due to the randomness during training sessions. This randomness occurs due to four reasons: i) training data shuffling, ii) random weight initialization of the models before training, iii) random FGSM perturbation size of adversarial sample generation for each batch in every epoch, and iv) random PGD iteration of adversarial sample generation for each batch in every epoch.

Moreover, our proposed approach suffers from robust accuracy degradation, when faces stronger attacks, which is very common among all other competitors. We can see that our proposed model outperforms all other

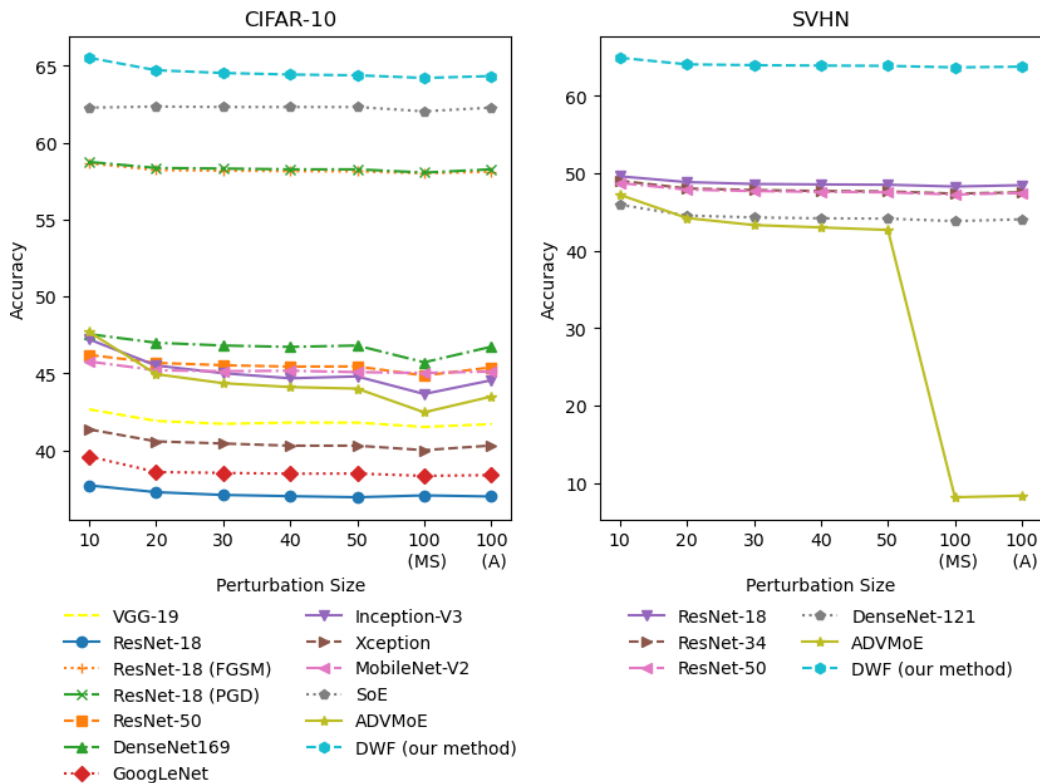


Figure 7: Robustness of our proposed model vs. other models against PGD w.r.t. different iteration numbers.

competitors in terms of robustness under all attacks. Additionally, DWF consistently outperforms existing defenses such as ADVMoE, SoE, and adversarially trained networks in terms of clean accuracy. Notably, it maintains a clean accuracy above 90% across both datasets, highlighting its effectiveness not only against adversarial attacks but also in non-adversarial environments. Compared to plain (undefended) networks, DWF exhibits at most a modest reduction in clean accuracy, which is expected since DWF incorporates adversarial training and jointly optimizes robustness-oriented objectives through the gating mechanism and expert updates. This optimization slightly shifts capacity toward worst-case robustness, whereas plain models are optimized purely for benign performance. Importantly, the clean accuracy drop in DWF is noticeably smaller than in standard adversarially trained baselines, indicating that the mixture-of-experts design helps preserve discriminative

capacity on benign inputs while still providing substantial robustness gains.

Moreover, the results demonstrate that our method could preserve its performance under adaptive white-box scenario, suggesting that the resilience does not stem from gradient masking/obfuscation. Another insight illustrates that as we increase perturbation size or iterations in FGSM and PGD, the robustness of all other models drops, which shows the lack of adaptability of the models against attacks with more extreme specifications. As a result, it is useful to consider how the gating mechanism may behave under stronger perturbations. In a soft-gated mixture-of-experts architecture, routing can distribute weights across multiple experts when predictions become uncertain, which may help avoid complete reliance on any single expert and lead to gradual performance degradation as attack strength increases. We focus on overall robustness trends in this work.

The robustness gains of DWF can be interpreted through several complementary mechanisms. First, multiple experts introduce functional diversity, which reduces correlated failure modes and makes adversarial transfer across experts more difficult. Second, soft gating enables input-dependent specialization, allowing each expert to focus on a subset of the data manifold and improving local decision boundaries. Third, joint optimization with adversarial training encourages smoother and more stable gradients across the mixture. Together, these effects contribute to improved robustness without a large sacrifice in clean accuracy.

6. Conclusion and Future Works

In this study, we evaluated DWF’s robustness primarily under white-box attacks, which represent the strongest and most conservative threat model since the adversary has full access to the model parameters and gradients. Robustness under white-box optimization is widely regarded as a lower bound on performance under weaker settings, such as transfer-based or query-limited black-box attacks, which typically yield higher robust accuracy. Therefore, defenses that remain effective in the white-box scenario are expected to generalize well to these weaker threat models. A systematic evaluation of DWF under transfer and black-box attacks is an interesting direction for future work.

DWF integrates several complementary mechanisms, including soft gating, fractional expert activation, joint expert-gating optimization, and randomized adversarial training. Each component addresses a distinct limitation of

conventional defenses. Soft gating enables input-dependent expert specialization, fractional activation reduces overfitting and improves diversity, joint updating ensures coordinated optimization between experts and routing, and randomized adversarial training improves robustness across varying perturbation strengths. Together, these components contribute synergistically to both clean and robust accuracy. Conducting a full combinatorial ablation over all variants would require retraining numerous MoE configurations with substantial computational cost; therefore, we leave a comprehensive ablation study for future work.

While this work focuses primarily on improving robustness, training efficiency is also an important practical consideration. Fast adversarial training variants (e.g., FFAT or single-step approximations) may reduce computational cost at the expense of some robustness. A systematic study quantifying the trade-off between training time and robust accuracy for DWF under different efficient training strategies would require multiple full training runs and extensive hyperparameter tuning. We leave this investigation for future work. Moreover, We trained and tested our model against two popular attacks, FGSM and PGD. To further expand our method one can train and evaluate the model on a wider range of adversarial attacks.

Although the proposed framework is evaluated on image classification tasks, the soft-gated mixture-of-experts design is largely architecture-agnostic and can, in principle, be integrated with other modalities such as text, speech, or time-series models. The core idea of training specialized experts and adaptively routing inputs through a gating network does not depend on convolutional backbones. However, extending the method to other domains may require modality-specific adversarial threat models and training strategies, and could introduce additional computational costs. Exploring these extensions is an interesting direction for future work.

References

- [1] A. A. Khan, A. A. Laghari, and S. A. Awan, “Machine learning in computer vision: A review.,” *EAI Endorsed Transactions on Scalable Information Systems*, vol. 8, no. 32, 2021.
- [2] A. I. Khan and S. Al-Habsi, “Machine learning in computer vision,” *Procedia Computer Science*, vol. 167, pp. 1444–1451, 2020.
- [3] H. Habehh and S. Gohel, “Machine learning in healthcare,” *Current genomics*, vol. 22, no. 4, pp. 291–300, 2021.

- [4] A. Qayyum, J. Qadir, M. Bilal, and A. Al-Fuqaha, “Secure and robust machine learning for healthcare: A survey,” *IEEE Reviews in Biomedical Engineering*, vol. 14, pp. 156–180, 2020.
- [5] I. Lauriola, A. Lavelli, and F. Aioli, “An introduction to deep learning in natural language processing: Models, techniques, and tools,” *Neurocomputing*, vol. 470, pp. 443–456, 2022.
- [6] M. Omar, S. Choi, D. Nyang, and D. Mohaisen, “Robust natural language processing: Recent advances, challenges, and future directions,” *IEEE Access*, vol. 10, pp. 86038–86056, 2022.
- [7] H. Jelodar, M. Meymani, and R. Razavi-Far, “Large language models (llms) for source code analysis: applications, models and datasets,” *arXiv preprint arXiv:2503.17502*, 2025.
- [8] G. Apruzzese, P. Laskov, E. Montes de Oca, W. Mallouli, L. Brdalo Rapa, A. V. Grammatopoulos, and F. Di Franco, “The role of machine learning in cybersecurity,” *Digital Threats: Research and Practice*, vol. 4, no. 1, pp. 1–38, 2023.
- [9] Y. Xin, L. Kong, Z. Liu, Y. Chen, Y. Li, H. Zhu, M. Gao, H. Hou, and C. Wang, “Machine learning and deep learning methods for cybersecurity,” *Ieee access*, vol. 6, pp. 35365–35381, 2018.
- [10] A. L. Buczak and E. Guven, “A survey of data mining and machine learning methods for cyber security intrusion detection,” *IEEE Communications surveys & tutorials*, vol. 18, no. 2, pp. 1153–1176, 2015.
- [11] N. Pitropakis, E. Panaousis, T. Giannetsos, E. Anastasiadis, and G. Loukas, “A taxonomy and survey of attacks against machine learning,” *Computer Science Review*, vol. 34, p. 100199, 2019.
- [12] P. Bountakas, A. Zarras, A. Lekidis, and C. Xenakis, “Defense strategies for adversarial machine learning: A survey,” *Computer Science Review*, vol. 49, p. 100573, 2023.
- [13] A. Kurakin, I. Goodfellow, and S. Bengio, “Adversarial machine learning at scale,” *arXiv preprint arXiv:1611.01236*, 2016.
- [14] D. Kaur, S. Uslu, K. J. Rittichier, and A. Durrezi, “Trustworthy artificial intelligence: a review,” *ACM computing surveys (CSUR)*, vol. 55, no. 2, pp. 1–38, 2022.
- [15] Y. LeCun, L. Bottou, Y. Bengio, and P. Haffner, “Gradient-based learning applied to document recognition,” *Proceedings of the IEEE*, vol. 86, no. 11, pp. 2278–2324, 2002.
- [16] Bipartisan House Task Force on Artificial Intelligence, “Leading ai progress: Policy insights and a u.s. vision for ai adoption, responsible innovation, and governance,” 2024. Report of the Bipartisan House AI Task Force, 118th Congress.

- [17] D. Kusnezov, Y. Barsoum, E. Begoli, A. Henninger, and A. Sadovnik, “Risks and mitigation strategies for adversarial artificial intelligence threats: A dhs s&t study preparedness series,” 06 2023.
- [18] S. Mu and S. Lin, “A comprehensive survey of mixture-of-experts: Algorithms, theory, and applications,” *arXiv preprint arXiv:2503.07137*, 2025.
- [19] W. Cai, J. Jiang, F. Wang, J. Tang, S. Kim, and J. Huang, “A survey on mixture of experts in large language models,” *IEEE Transactions on Knowledge and Data Engineering*, 2025.
- [20] J. Puigcerver, C. Riquelme, B. Mustafa, and N. Houlsby, “From sparse to soft mixtures of experts,” *arXiv preprint arXiv:2308.00951*, 2023.
- [21] M. Bakirci, “A novel swarm unmanned aerial vehicle system: Incorporating autonomous flight, real-time object detection, and coordinated intelligence for enhanced performance.,” *Traitement du Signal*, vol. 40, no. 5, 2023.
- [22] C. Lin, S. Han, J. Zhu, Q. Li, C. Shen, Y. Zhang, and X. Guan, “Sensitive region-aware black-box adversarial attacks,” *Information Sciences*, vol. 637, p. 118929, 2023.
- [23] Y. Gong, S. Wang, T. Yu, X. Jiang, and F. Sun, “Improving adversarial robustness using knowledge distillation guided by attention information bottleneck,” *Information Sciences*, vol. 665, p. 120401, 2024.
- [24] I. J. Goodfellow, J. Shlens, and C. Szegedy, “Explaining and harnessing adversarial examples,” *arXiv preprint arXiv:1412.6572*, 2014.
- [25] A. Madry, A. Makelov, L. Schmidt, D. Tsipras, and A. Vladu, “Towards deep learning models resistant to adversarial attacks,” *arXiv preprint arXiv:1706.06083*, 2017.
- [26] N. Carlini and D. Wagner, “Towards evaluating the robustness of neural networks,” in *2017 IEEE Symposium on Security and Privacy (SP)*, pp. 39–57, Ieee, 2017.
- [27] Z. Tian, L. Cui, J. Liang, and S. Yu, “A comprehensive survey on poisoning attacks and countermeasures in machine learning,” *ACM Computing Surveys*, vol. 55, no. 8, pp. 1–35, 2022.
- [28] Y. Bai, G. Xing, H. Wu, Z. Rao, C. Ma, S. Wang, X. Liu, Y. Zhou, J. Tang, K. Huang, *et al.*, “Backdoor attack and defense on deep learning: A survey,” *IEEE Transactions on Computational Social Systems*, 2024.
- [29] S. Zhang, W. Chen, X. Li, Q. Liu, and G. Wang, “Apbam: Adversarial perturbation-driven backdoor attack in multimodal learning,” *Information Sciences*, vol. 700, p. 121847, 2025.
- [30] J. Zheng, P. P. Chan, H. Chi, and Z. He, “A concealed poisoning attack to reduce deep neural networks’ robustness against adversarial samples,” *Information Sciences*, vol. 615, pp. 758–773, 2022.

- [31] M. Rigaki and S. Garcia, “A survey of privacy attacks in machine learning,” *ACM Computing Surveys*, vol. 56, no. 4, pp. 1–34, 2023.
- [32] Z. Zhang, J. Ma, X. Ma, R. Yang, X. Wang, and J. Zhang, “Defending against membership inference attacks: Rm learning is all you need,” *Information Sciences*, vol. 670, p. 120636, 2024.
- [33] R. Shokri, M. Stronati, C. Song, and V. Shmatikov, “Membership inference attacks against machine learning models,” in *2017 IEEE symposium on security and privacy (SP)*, pp. 3–18, IEEE, 2017.
- [34] F. Regazzoni, S. Bhasin, A. A. Pour, I. Alshaer, F. Aydin, A. Aysu, V. Beroulle, G. Di Natale, P. Franzon, D. Hely, *et al.*, “Machine learning and hardware security: Challenges and opportunities,” in *Proceedings of the 39th International Conference on Computer-Aided Design*, pp. 1–6, 2020.
- [35] B. Hettwer, S. Gehrler, and T. Güneysu, “Applications of machine learning techniques in side-channel attacks: a survey,” *Journal of Cryptographic Engineering*, vol. 10, no. 2, pp. 135–162, 2020.
- [36] T. Bai, J. Luo, J. Zhao, B. Wen, and Q. Wang, “Recent advances in adversarial training for adversarial robustness,” *arXiv preprint arXiv:2102.01356*, 2021.
- [37] M. Zhao, L. Zhang, J. Ye, H. Lu, B. Yin, and X. Wang, “Adversarial training: A survey,” *arXiv preprint arXiv:2410.15042*, 2024.
- [38] Z. Zhang, H. Xia, Z. Kang, R. Zhang, and X. Shi, “Catil: Customized adversarial training based on instance loss,” *Information Sciences*, vol. 689, p. 121420, 2025.
- [39] S. Jiang, Z. Wu, H. Yang, K. Xiang, W. Ding, and Z.-S. Chen, “A prior knowledge-guided distributionally robust optimization-based adversarial training strategy for medical image classification,” *Information Sciences*, vol. 673, p. 120705, 2024.
- [40] H. Zhang, Y. Yu, J. Jiao, E. Xing, L. El Ghaoui, and M. Jordan, “Theoretically principled trade-off between robustness and accuracy,” in *International conference on machine learning*, pp. 7472–7482, PMLR, 2019.
- [41] H. Xu, X. Liu, Y. Li, A. Jain, and J. Tang, “To be robust or to be fair: Towards fairness in adversarial training,” in *International conference on machine learning*, pp. 11492–11501, PMLR, 2021.
- [42] A. Shafahi, M. Najibi, M. A. Ghiasi, Z. Xu, J. Dickerson, C. Studer, L. S. Davis, G. Taylor, and T. Goldstein, “Adversarial training for free!,” *Advances in neural information processing systems*, vol. 32, 2019.
- [43] G. Apruzzese, M. Andreolini, M. Colajanni, and M. Marchetti, “Hardening random forest cyber detectors against adversarial attacks,” *IEEE Transactions on Emerging Topics in Computational Intelligence*, vol. 4, no. 4, pp. 427–439, 2020.

- [44] X. Tang, S. Mahloujifar, L. Song, V. Shejwalkar, M. Nasr, A. Houmansadr, and P. Mittal, “Mitigating membership inference attacks by {Self-Distillation} through a novel ensemble architecture,” in *31st USENIX security symposium (USENIX security 22)*, pp. 1433–1450, 2022.
- [45] G. Apruzzese, M. Andreolini, M. Marchetti, V. G. Colacino, and G. Russo, “Appcon: Mitigating evasion attacks to ml cyber detectors,” *Symmetry*, vol. 12, no. 4, p. 653, 2020.
- [46] A. Salem, Y. Zhang, M. Humbert, P. Berrang, M. Fritz, and M. Backes, “ML-leaks: Model and data independent membership inference attacks and defenses on machine learning models,” *arXiv preprint arXiv:1806.01246*, 2018.
- [47] T. Strauss, M. Hanselmann, A. Junginger, and H. Ulmer, “Ensemble methods as a defense to adversarial perturbations against deep neural networks,” *arXiv preprint arXiv:1709.03423*, 2017.
- [48] J. Puigcerver, R. Jenatton, C. Riquelme, P. Awasthi, and S. Bhojanapalli, “On the adversarial robustness of mixture of experts,” *Advances in neural information processing systems*, vol. 35, pp. 9660–9671, 2022.
- [49] S. Pavlitska, E. Eisen, and J. M. Zöllner, “Towards adversarial robustness of model-level mixture-of-experts architectures for semantic segmentation,” in *2024 International Conference on Machine Learning and Applications (ICMLA)*, pp. 1460–1465, IEEE, 2024.
- [50] Q. Han, Y. Zhai, Y. Qin, Y. Yang, *et al.*, “Enhancing the "immunity" of mixture-of-experts networks for adversarial defense,” *arXiv preprint arXiv:2402.18787*, 2024.
- [51] X. Zhang, K. Xu, Z. Hu, and R. Wang, “Optimizing robustness and accuracy in mixture of experts: A dual-model approach,” *arXiv preprint arXiv:2502.06832*, 2025.
- [52] Y. Zhang, R. Cai, T. Chen, G. Zhang, H. Zhang, P.-Y. Chen, S. Chang, Z. Wang, and S. Liu, “Robust mixture-of-expert training for convolutional neural networks,” in *Proceedings of the IEEE/CVF International Conference on Computer Vision*, pp. 90–101, 2023.
- [53] S. Cui, J. Zhang, J. Liang, B. Han, M. Sugiyama, and C. Zhang, “Synergy-of-experts: Collaborate to improve adversarial robustness,” *Advances in Neural Information Processing Systems*, vol. 35, pp. 32552–32567, 2022.
- [54] A. Krizhevsky, G. Hinton, *et al.*, “Learning multiple layers of features from tiny images,” 2009.
- [55] Y. Netzer, T. Wang, A. Coates, A. Bissacco, B. Wu, A. Y. Ng, *et al.*, “Reading digits in natural images with unsupervised feature learning,” in *NIPS workshop on deep learning and unsupervised feature learning*, vol. 2011, p. 7, Granada, 2011.

- [56] K. Liu, “pytorch-cifar.” <https://github.com/kuangliu/pytorch-cifar>, 2017.
- [57] F. Juraev, “Trained models for cifar-10 dataset.” <https://www.kaggle.com/datasets/firuzjuraev/trained-models-for-cifar10-dataset/data>, 2022.
- [58] E. Dadalto, “edadaltocg.” <https://huggingface.co/edadaltocg>, 2023.
- [59] K. Simonyan and A. Zisserman, “Very deep convolutional networks for large-scale image recognition,” *arXiv preprint arXiv:1409.1556*, 2014.
- [60] K. He, X. Zhang, S. Ren, and J. Sun, “Deep residual learning for image recognition,” in *Proceedings of the IEEE conference on computer vision and pattern recognition*, pp. 770–778, 2016.
- [61] G. Huang, Z. Liu, L. Van Der Maaten, and K. Q. Weinberger, “Densely connected convolutional networks,” in *Proceedings of the IEEE conference on computer vision and pattern recognition*, pp. 4700–4708, 2017.
- [62] C. Szegedy, V. Vanhoucke, S. Ioffe, J. Shlens, and Z. Wojna, “Rethinking the inception architecture for computer vision,” in *Proceedings of the IEEE conference on computer vision and pattern recognition*, pp. 2818–2826, 2016.
- [63] F. Chollet, “Xception: Deep learning with depthwise separable convolutions,” in *Proceedings of the IEEE conference on computer vision and pattern recognition*, pp. 1251–1258, 2017.
- [64] M. Sandler, A. Howard, M. Zhu, A. Zhmoginov, and L.-C. Chen, “Mobilenetv2: Inverted residuals and linear bottlenecks,” in *Proceedings of the IEEE conference on computer vision and pattern recognition*, pp. 4510–4520, 2018.
- [65] I. Loshchilov and F. Hutter, “Sgdr: Stochastic gradient descent with warm restarts,” *arXiv preprint arXiv:1608.03983*, 2016.